



NASA CR-114⁵25

ASRL TR 166-4

Available to the Public.

INVESTIGATION OF SOME PARAMETERS AFFECTING THE STABILITY OF A HINGELESS HELICOPTER BLADE IN HOVER

(NASA-CR-114525) INVESTIGATION OF SOME PARAMETERS AFFECTING THE STABILITY OF A HINGELESS HELICOPTER BLADE IN HOVER (Massachusetts Inst. of Tech.) 19 p HC \$3.00	N73-16015 Unclas 62001
--	----------------------------------

Peretz Friedmann

AEROELASTIC AND STRUCTURES RESEARCH LABORATORY
DEPARTMENT OF AERONAUTICS AND ASTRONAUTICS
MASSACHUSETTS INSTITUTE OF TECHNOLOGY
CAMBRIDGE, MASSACHUSETTS 02139

August 1972

Prepared for

AMES DIRECTORATE

U.S. ARMY AIR MOBILITY RESEARCH AND DEVELOPMENT LABORATORY
AMES RESEARCH CENTER
MOFFETT FIELD, CALIFORNIA

Contract No. NAS2-6175

1. Report No. 5 NASA CR-114/25		2. Government Accession No.		3. Recipient's Catalog No.	
4. Title and Subtitle INVESTIGATION OF SOME PARAMETERS AFFECTING THE STABILITY OF A HINGELESS HELICOPTER BLADE				5. Report Date August 1972	
				6. Performing Organization Code	
7. Author(s) Peretz Friedmann				8. Performing Organization Report No. ASRL TR 166-4	
9. Performing Organization Name and Address Aeroelastic and Structures Research Laboratory Department of Aeronautics and Astronautics Massachusetts Institute of Technology Cambridge, Massachusetts 02139				10. Work Unit No.	
				11. Contract or Grant No. NAS2-6175	
12. Sponsoring Agency Name and Address Ames Directorate, U.S. Army Air Mobility Research and Development Laboratory Ames Research Center, Moffett Field, California 94035				13. Type of Report and Period Covered Contractor Report	
				14. Sponsoring Agency Code	
15. Supplementary Notes Technical Monitor: Dr. R.A. Ormiston, Ames Directorate, U.S. Army Air Mobility Research and Development Laboratory, Ames Research Center, Moffett Field, California 94035					
16. Abstract In this report, the equations of motion derived in Ref. 1 are used to investigate the effects of the choice of the mode shape and built-in coning angle β_p on the stability boundaries of hingeless blades in hover. The results obtained indicate that the stability boundaries are dependent upon the mode shape to a considerable degree. It was also found that positive built-in coning is usually destabilizing while a negative amount of built-in coning can be quite stabilizing.					
17. Key Words (Suggested by Author(s)) Helicopter Aeroelasticity Rotor Blade Dynamics Rotor Blade Flutter Nonlinear Blade Dynamics Dynamic Stability				18. Distribution Statement Unclassified, Unlimited	
19. Security Classif. (of this report) Unclassified		20. Security Classif. (of this page) Unclassified		21. No. of Pages 18	22. Price* \$3.00

* For sale by the National Technical Information Service, Springfield, Virginia 22151

FOREWORD

This research was conducted by the Aeroelastic and Structures Research Laboratory, Department of Aeronautics and Astronautics, Massachusetts Institute of Technology, Cambridge, Massachusetts under Contract No. NAS2-6175, supervised by Dr. R.A. Ormiston of the Ames Directorate, U.S. Army Air Mobility Research and Development Laboratory, Ames Research Center, Moffett Field, California.

The author wishes to express his appreciation to Dr. R.A. Ormiston for his useful comments and suggestions.

The author is deeply indebted to Professors R.H. Miller, N.D. Ham, and E.A. Witmer for their extremely helpful advice and constructive criticism in the course of this study.

The digital computations were carried out at the MIT Information Processing Center.

CONTENTS

<u>Section</u>		<u>Page</u>
1	INTRODUCTION	1
2	EQUATIONS OF MOTION, STABILITY BOUNDARIES, AND COMPUTER PROGRAMS USED	1
	2.1 The Linearized Equations	1
	2.2 The Nonlinear Equations	1
	2.3 The Stability Boundaries	1
	2.4 Computer Programs	2
3	RESULTS AND DISCUSSION	2
	3.1 Effect of Mode Shape on the Stability Boundaries	2
	3.1.1 Introductory Remarks	2
	3.1.2 Remarks Concerning the Use of Young's Blade Model in the Present Report	4
	3.1.3 Effect of the Mode Shape on the Divergence Boundaries	5
	3.1.4 Effect of the Mode Shape on the Flap-Lag Stability Boundaries	5
	3.1.5 The Effect of the Mode Shape on the Flap- Pitch Stability Boundary	6
	3.2 Effect of Built-In Coning β_p on the Stability Boundaries	7
	3.2.1 Effect of Built-In Coning on the Flap-Pitch Stability Boundary	8
	3.2.2 Effect of Built-In Coning on the Flap- Lag-Type of Stability Boundary	8
	3.3 Numerical Integration of the Coupled Nonlinear Flap-Lag-Pitch Equations of Motion in Hover	9
4	CONCLUSIONS	9
	REFERENCES	10
	FIGURES	11

LIST OF ILLUSTRATIONS

<u>Figure</u>		<u>Page</u>
1	Effect of the Mode Shape on the Flap-Lag Stability Boundaries	11
2	Effect of the Mode Shape on the Flap-Pitch Stability Boundary	12
3	Effect of Built-In Coning on the Flap-Pitch Stability Boundary	13
4	Effect of Built-In Coning on the Flap-Lag-Type of Stability Boundary	14

1. INTRODUCTION

In Ref. 1, it was indicated that the stability boundaries could be mode-shape dependent. It was also suggested that the equations of Ref. 1 could be used as a basis for a parametric investigation from which an optimum blade configuration from the flutter point of view could be defined. Due to the limited amount of time available for the preparation of this report, it was decided to limit the study to the investigation of the effect of the mode shape on the flap-lag and flap-pitch stability boundaries together with the effect of the built-in coning β_p on the stability of hingeless blades. The study was performed using the equations of motion, stability boundaries, and computer programs described in detail in Ref. 1. The important effect of elastic coupling on these stability boundaries was neglected, for reasons similar to those given in Ref. 1.

2. EQUATIONS OF MOTION, STABILITY BOUNDARIES, AND COMPUTER PROGRAMS USED

2.1 The Linearized Equations

The linearized equations of motion for coupled flap-lag-pitch motion of a hingeless blade in hover are given in Ref. 1, Eqs. 9.24, 9.25, and 9.27. The various flutter derivatives used in these equations are defined by the appropriate relations in Appendix N of Ref. 1.

2.2 The Nonlinear Equations

The complete nonlinear equations for coupled flap-lag-pitch motion of a hingeless blade in hover are given by Eqs. 9.28 through 9.30 of Ref. 1. The flutter derivatives and the appropriate nonlinear functions which are to be used with these equations are given in Appendices N and O of Ref. 1.

2.3 The Stability Boundaries

The static stability boundaries used in this report are the "approximate divergence boundaries" defined by Eqs. 10.1 through 10.3 of Ref. 1.

The dynamic stability or flutter boundaries for flap-lag, flap-pitch, and coupled flap-lag-pitch are given, respectively, by Eqs. 4.4, 4.5, 10.12, and 10.6 of Ref. 1.

2.4 Computer Programs

The computer programs used for evaluating the divergence and flutter boundaries were those described in Ref. 1.

A new computer program has been developed for integrating the nonlinear coupled flap-lag-pitch equations of motion in hover using the predictor-corrector method.

3. RESULTS AND DISCUSSION

3.1 Effect of Mode Shape on the Stability Boundaries

3.1.1 Introductory Remarks

As pointed out in conclusion No. 1 of Subsection 12.2 in Ref. 1, the stability boundaries obtained could be quite sensitive to the assumed mode shape because the various coefficients which appear in the equations of motion (representing generalized masses and forces) are themselves mode-shape dependent. It was also implied in Ref. 1 that the static equilibrium position of the blade, which is dependent upon the assumed mode shape, could have a considerable effect on the location of the stability boundaries.

In Ref. 1, an assumed mode shape given by

$$\eta_1 = \left(-\frac{1}{3}\right) [1 - 4\bar{x}_0 - (1 - \bar{x}_0)^4] \quad (1)$$

was used. Where η_1 is the first flapwise normal bending mode, $\bar{x}_0 = (x - e_1)/\ell$, ℓ is the length of the blade capable of elastic deflection and e_1 is an offset. The geometry of the problem is shown in Figs. 1 and 27 of Ref. 1. The mode shape represented by Eq. 1 closely resembles the first mode shape of a nonrotating cantilever beam. It was also assumed that the mode shape in flap is the same as the mode shape in lag. Inherent in the analysis of Ref. 1 is the assumption that the mode shape is unaffected by the rotation of the blade and the first rotating flap or lag frequency is obtained by a process analogous to the classical Southwell coefficient (Appendix A, Ref. 1). All cases treated in Ref. 1 had constant mass and stiffness distributions along the span of the blade.

It seemed therefore reasonable to investigate how the stability boundaries

obtained in Ref. 1 will be affected by other representations of the mode shape. Various approaches for modelling the first mode shape in flap (or lag) of a hingeless blade are feasible:

- (1) Assume that the first and higher rotating mode shapes can be represented by a series of nonrotating mode shapes. The use of Galerkin's method to solve this free-vibration problem of a rotating beam will yield the first (and higher) rotating mode shapes and frequencies. This approach has been used in Ref. 2. For uniform mass and stiffness distribution, it was found in Ref. 2 that the first and second bending mode shapes may change appreciably with the rotational speed.

Using the rotating mode shape obtained from this type of analysis as an input for the calculation of the flutter boundaries could yield reasonably accurate boundaries. The drawback in using this method in a trend-type-study such as Ref. 1 is due to the fact that for each point on the flutter boundary, a mass and stiffness distribution must be specified, together with a certain speed of rotation. Thus, first an eigenvalue problem must be solved to obtain the rotating mode shape and then the flutter boundary point must be obtained. This procedure implies the recomputation of the generalized mass and force coefficients, defined in Appendices B, C, and M of Ref. 1 for each point along the flutter boundary. Such a procedure will increase the computing time required to obtain a point on the flutter boundary by a factor of three (approximately).

- (2) Use Young's offset hinged spring restrained representation of the hingeless blade as derived in Ref. 3 and used in Ref. 4. According to Young, a reasonable representation of the first modal bending of a hingeless blade may be obtained by a rigid articulated blade restrained

about its offset flapping hinge by a torsional spring whose stiffness matches the first nonrotating frequency of the hingeless blade and the offset is such that the two systems have the same rotating frequency. This model was used in Ref. 4 for stability and control calculations of helicopters having hingeless blades, with the conclusion that it can be used as an approximate representation for blades with uniform mass and stiffness distribution.

- (3) Another approximate representation of the hingeless blade has been suggested in Ref. 5 by Bramwell. Bramwell's model is based upon the assumption that the elastic term in the free vibration equation representing the flap-bending motion of a rotating cantilever beam is negligible when compared with the centrifugal term. With this assumption an approximate geometric hinge offset can be defined using only the first rotating frequency of the blade. As pointed out in Ref. 5, this approximation is quite good for a particular type of hingeless blade which has its stiffness (and mass) concentrated near the root.

When choosing one of the three methods mentioned above, it is clear that the best method to use is method (1). Unfortunately, due to various time limitations, it could not be adopted and it was decided to use Young's method for the hingeless blade because it is superior to Bramwell's for uniform mass and stiffness distribution.

3.1.2 Remarks Concerning the Use of Young's Blade Model in the Present Report

In using Young's offset-hinged spring-restrained model for the hingeless blade, the quantity ℓ/R (ℓ - length of blade capable of elastic deflection, R - radius of the blade tip path) was always taken as equal to 1, and the mode shape in both flap and lag was assumed to be defined by the following relations ($\bar{e}_1 = 0$, $x_0 = x$):

$$\eta_1 = 0 \quad \text{for } 0 < \bar{x} < \bar{e}$$

$$\eta_1 = \frac{x_o - \bar{l}}{1 - \bar{e}} \quad \text{for } \bar{e} < \bar{x} < 1$$

where $\bar{e} = e/R$ is the offset used in representing the blade by Young's model.

The correct use of Young's model for a hingeless blade would require a different value of the offset e for the mode shape in flap and the mode shape in lag. In addition, these values of the offsets should be changed when moving from one point on the stability boundary to another one.

In Ref. 1, the same assumed mode shape was used for both flap and lag. Thus, in order to evaluate the effect of the mode shape on the stability boundaries of Ref.1, the same value of the offset e was used in both the flap and lag direction. It was also assumed that the offset e is fixed for a whole stability boundary plot. This is equivalent to using the same assumed mode shape (Eq. 1) for a whole stability boundary.

Due to the assumptions mentioned above, the results which will be presented should be considered to be illustrations indicating trends and not accurate stability boundaries for a particular blade.

3.1.3 Effect of the Mode Shape on the Divergence Boundaries

In order to obtain the effect of the assumed mode shape on the linearized approximate divergence boundaries (Eqs. 10.1 through 10.3 of Ref. 1), Fig. 33 of Ref. 1 was recalculated for two values of \bar{e} : $\bar{e} = .15$ and $\bar{e} = .20$. It was found that the approximate divergence boundaries were almost completely unaffected by the mode shape. The reason is probably due to the fact that the approximate divergence boundaries are, by definition, independent of the initial flap, lag, and torsional amplitudes (denoted by g_1^o , h_1^o , and ϕ_o , respectively, in Ref. 1) which are the quantities influenced by changing the mode shape.

3.1.4 Effect of the Mode Shape on the Flap-Lag Stability Boundaries

To illustrate this effect, the flutter boundary in flap-lag for $\theta_c = .20$ (Fig. 4, Ref. 1) was recomputed using two different values of \bar{e} : $\bar{e} = .15$ and

$\bar{e} = .20$. The inflow relation used for calculating this stability boundary is given by Eq. 5.5 of Ref. 1. The results obtained are shown in Fig. 1; the notation used in the figure is defined below:

$a = 2\pi$ = two-dimensional lift-curve slope

C_{d_o} = profile drag coefficient

σ = blade solidity

γ = Locke number

η_{SF1}, η_{SL1} = structural damping in flap and lag, respectively

$\bar{\omega}_{F1}$ = first rotating flap frequency nondimensionalized with respect to Ω

$\bar{\omega}_{L1}$ = first rotating lag frequency nondimensionalized with respect to Ω

Ω = speed of rotation of the blade

θ_c = the critical value of collective pitch setting above which the blade is unstable in flap-lag

The unstable regions are the combinations of rotating flap and lag frequencies which lie inside the ellipse-like stability boundary. Figure 1 shows the effect of the mode shape on the stability boundary. Different values of \bar{e} can be considered to represent different mode shapes. As can be seen, decreasing \bar{e} reduces the unstable areas inside the stability boundary.

Although the purpose of the curves is only to illustrate that the stability boundaries are mode-shape sensitive, one can still conclude that this indicates that in calculating stability boundaries which are to be used for design purposes, the correct rotating mode shape should be used to get a representative stability boundary.

3.1.4 The Effect of the Mode Shape on the Flap-Pitch Stability Boundary

In order to illustrate the effect of the mode shape on the flap-pitch stability boundary, Fig. 40 of Ref. 1 was recalculated for two values of the nondimensional hinge offset \bar{e} : $\bar{e} = .15$ and $\bar{e} = .20$.

The stability boundaries shown in Fig. 2 were evaluated using the inflow given by Eq. 7.3 of Ref. 1. For the sake of completeness, the notation used in Fig. 2 is defined below:

- θ_c = critical collective pitch setting above which the blade is unstable in flap pitch
- $\bar{\omega}_o$ = torsional frequency nondimensionalized with respect to Ω
- b = blade half-chord nondimensionalized with respect to Ω
- $I = I_f/I_o$ = inertia ratio
- I_o = polar moment of inertia of the whole blade
- I_b = mass moment of inertia of the elastic part of the blade about its root, defined in Appendix B, Ref. 1

Again, Fig. 2 shows that the stability boundaries in flap-pitch are mode-shape sensitive.

It is of interest to note that for both the flap-lag and flap-pitch-type of instability, decreasing the offset \bar{e} from .20 to .15 tends to decrease the unstable regions under the stability boundary.

3.2 Effect of Built-In Coning β_p on the Stability Boundaries

In Ref. 1, it was shown that the angle of built-in coning β_p (defined in Fig. 27b of Ref. 1) had a considerable effect on the divergence boundaries of a hingeless blade. Some hingeless blades have a certain amount of built-in coning in order to relieve blade stresses; therefore, it seemed reasonable to investigate the effect of built-in coning on the flap-lag and flap-pitch stability boundaries.

3.2.1 Effect of Built-In Coning on the Flap-Pitch Stability Boundary

This effect is illustrated by Fig. 3. The inflow for this calculation was evaluated using Eq. 7.3 of Ref. 1. The pertinent data for this calculation is given in Fig. 3. The collective pitch setting for this case was $\theta = .17$. As can be seen, a positive amount of built-in coning is slightly destabilizing for this type of instability. Around $\beta_p = 2^\circ$, this destabilizing effect is the strongest; beyond this value the destabilizing effect is somewhat weaker. On the other hand, a small amount of negative built-in coning is quite stabilizing for the flap-pitch-type of instability. From Fig. 3, a negative built-in coning angle of $\beta_p = - .65^\circ$ can considerably reduce the minimal torsional stiffness required for stability. Thus, built-in coning could be a possible simple method of stabilizing blades which have flap-pitch-type of stability problems. It is important to note again that this effect too, can be very much dependent upon the assumed mode shape, and the discussion of the previous section regarding mode shape effects on the stability boundary is applicable to this case also.

3.2.2 Effect of Built-In Coning on the Flap-Lag-Type of Stability Boundary

For simulating this effect, the coupled flap-lag-pitch program was used with a high value for the torsional stiffness, $\bar{\omega}_o = 100$, thus effectively eliminating the torsional degree of freedom. The effect of built-in coning was investigated for the following cases:

- (a) $\bar{\omega}_{F1} = 1.175$; $\bar{\omega}_{L1} = 1.075764$; $\bar{\omega}_o = 100$
(b) $\bar{\omega}_{F1} = 1.175$; $\bar{\omega}_{L1} = 1.28303$; $\bar{\omega}_o = 100$

These two cases correspond, respectively, to the lower and upper branch of the stability boundary points for $\theta_c = .20$ and $\bar{\omega}_{F1} = 1.175$ (Fig. 8, Ref. 1) with the inflow calculated from Eq. 7.3 of Ref. 1. The various other parameters used in the calculation are given in Fig. 4. For these two cases, the effect of β_p on the flutter boundary is quite similar and the two curves are coincident for all practical purposes. From the numerical values obtained, it was found

that the values of θ_c for the two curves agree up to the third decimal digit.

As can be seen from Fig. 4, positive values of β_p are strongly destabilizing for the flap-lag-type of instability. On the other hand, a small amount of negative built-in coning is quite stabilizing.

Again, it should be emphasized that these results are mode-shape dependent. In fact the stability boundary given in Fig. 4 was recalculated using Young's model for the hingeless blade with $\bar{e} = .20$ and from the results it was found that the effect of the mode shape is of the same magnitude as that illustrated by Fig. 1.

3.3 Numerical Integration of the Coupled Nonlinear Flap-Lag-Pitch Equations of Motion in Hover

A computer program was developed for integrating these nonlinear equations as explained in Subsections 2.2 and 2.4. Due to the limited amount of time available, only a small number of cases was considered. The results are inconclusive, although it seems that with the torsional degree of freedom in the equation, the limit cycle amplitudes are much smaller than those obtained for the flap-lag-type of instability considered in Ref. 1.

4. CONCLUSIONS

- (1) The stability boundaries in both flap-lag and flap-pitch are mode-shape dependent. Thus, in the calculation of stability boundaries which are to be used in hingeless blade design, the use of the exact rotating mode shape (or mode shapes) is recommended.
- (2) For the cases considered, positive built-in coning seems to have a minor destabilizing effect on the flap-pitch-type of instability, while a small amount of negative built-in coning is quite stabilizing.
- (3) For the cases considered, positive built-in coning has a strongly destabilizing effect on the flap-lag-type of instability, while negative built-in coning is quite stabilizing.

REFERENCES

1. Friedmann, P., and Tong, P., "Dynamic Nonlinear Elastic Stability of Helicopter Rotor Blades in Hover and in Forward Flight", Massachusetts Institute of Technology, Aeroelastic and Structures Research Laboratory Report, ASRL 166-3, June 1972.
2. Yntema, R.T., "Simplified Procedures and Charts for the Rapid Estimation of Bending Frequencies of Rotating Beams", NACA TN 3459, 1955.
3. Young, M.I., "A Simplified Theory of Hingeless Rotors with Application to Tandem Helicopters", 18th Annual Forum of the American Helicopter Society, 1962.
4. Shupe, N.K., "A Study of the Dynamic Motions of Hingeless Rotored Helicopters", ECOM-3323, Research and Development Technical Report, August 1970.
5. Bramwell, A.R.S., "A Method for Calculating the Stability and Control Derivatives of Helicopters with Hingeless Rotors", City University London, Research Memorandum Aero 69/4, 1969.

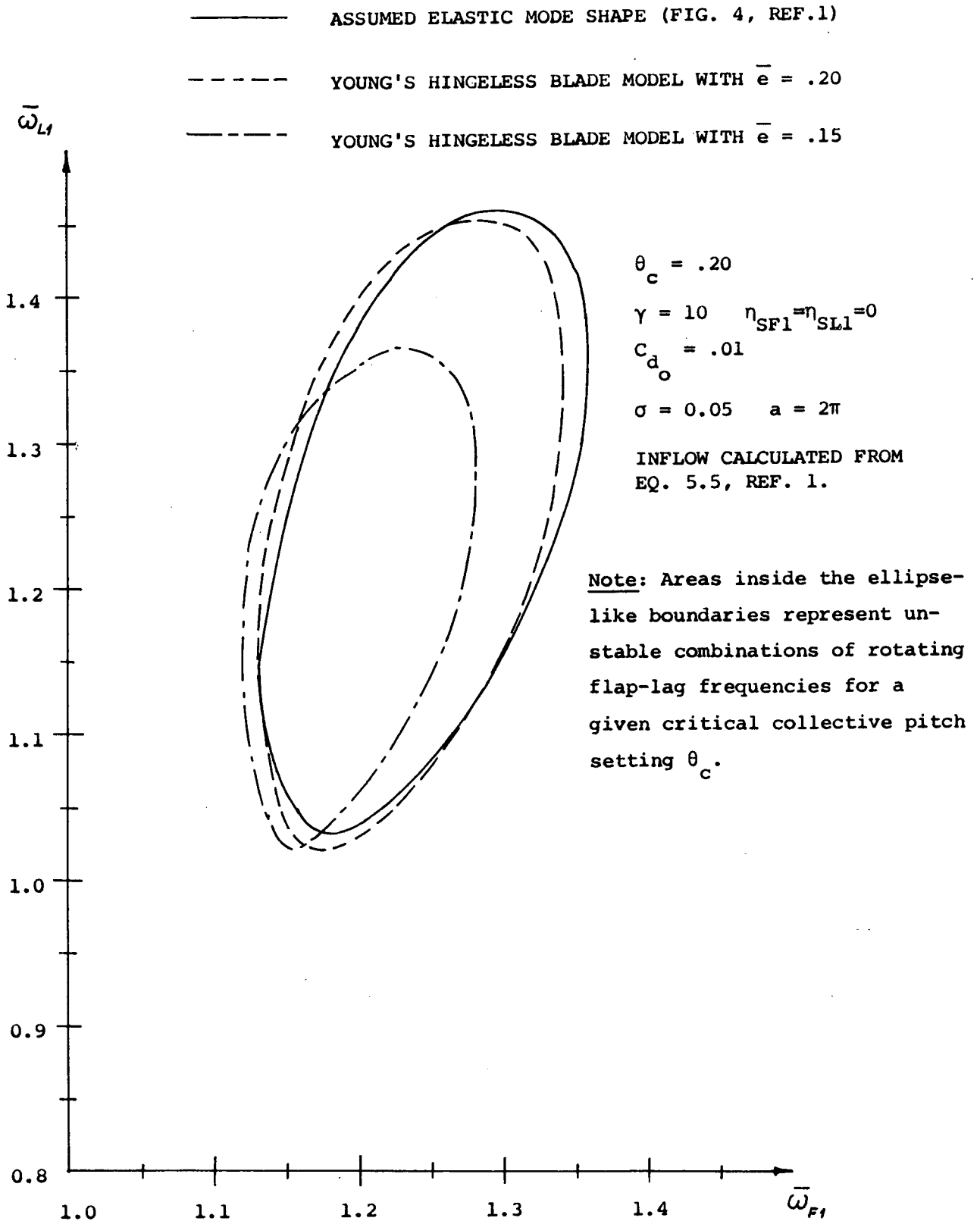


FIG. 1 EFFECT OF THE MODE SHAPE ON THE FLAP-LAG STABILITY BOUNDARIES

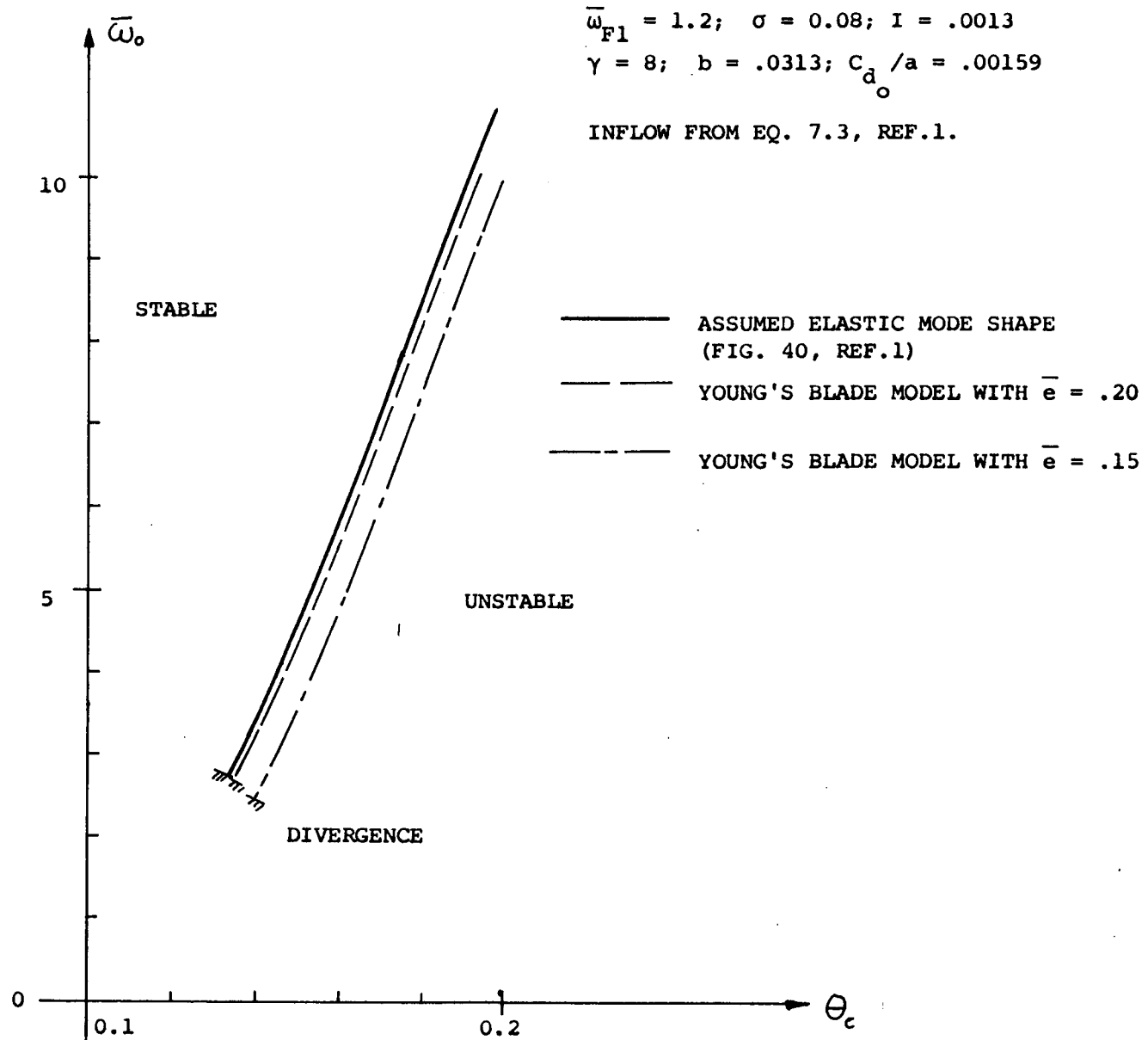


FIG. 2 EFFECT OF THE MODE SHAPE ON THE FLAP-PITCH STABILITY BOUNDARY

$$\bar{\omega}_{F1} = 1.2; \quad \sigma = 0.08; \quad \theta = .17; \quad I = .0013$$

$$b = .0313; \quad C_{d_o}/a = .00159; \quad \gamma = 8$$

INFLOW CALCULATED FROM EQ. 7.3, REF.1

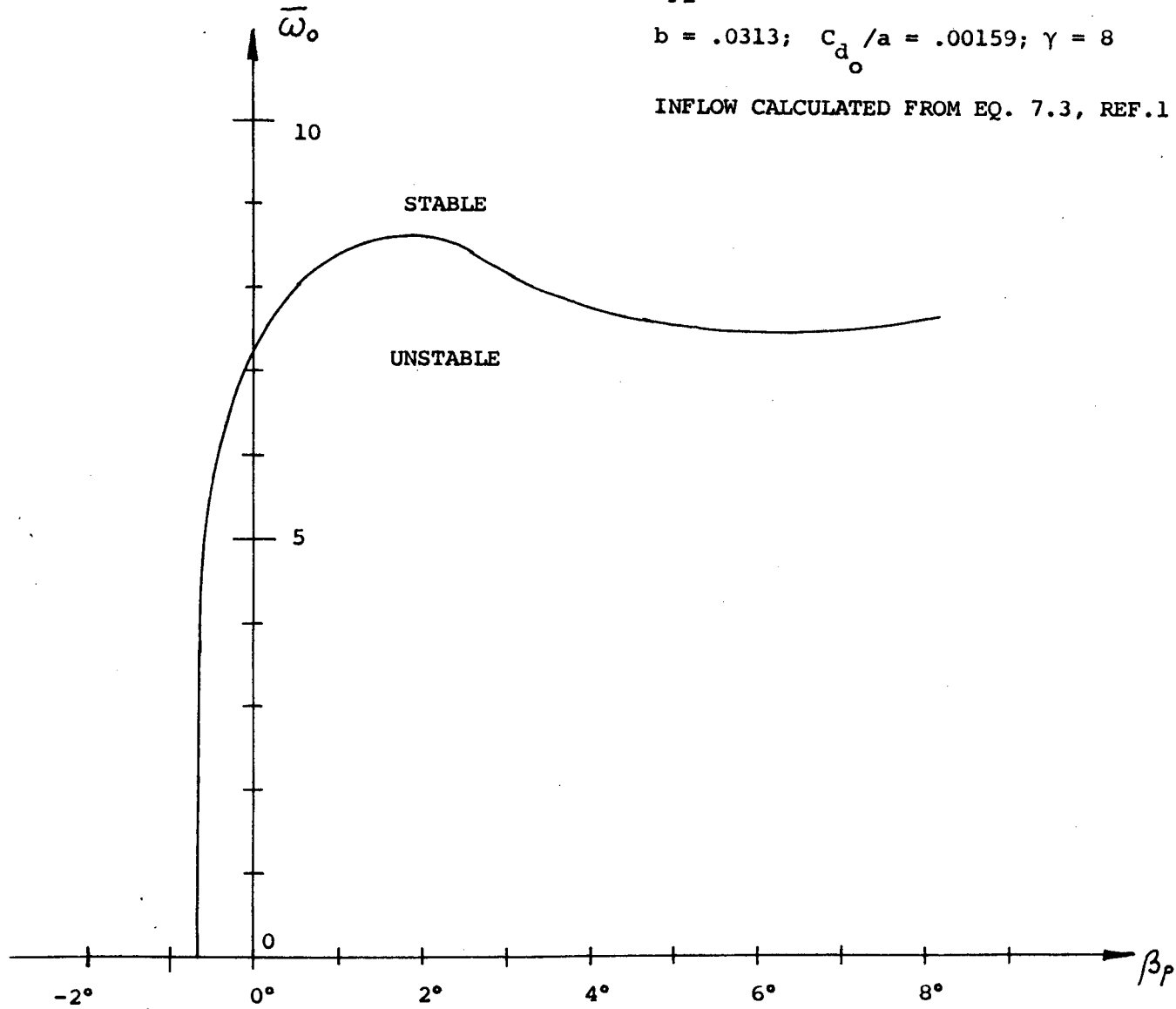


FIG. 3 EFFECT OF BUILT-IN CONING ON THE FLAP-PITCH STABILITY BOUNDARY

(a) $\bar{\omega}_{F1} = 1.175$; $\bar{\omega}_{L1} = 1.075764$; $\bar{\omega}_O = 100$

(b) $\bar{\omega}_{F1} = 1.175$; $\bar{\omega}_{L1} = 1.28303$; $\bar{\omega}_O = 100$

θ_c

REMARK: CURVES FOR THE TWO CASES ALMOST COINCIDE

$b = 0.025$ $c_{d_o}/a = .00159$ $\sigma = .05$ $I = .001$

INFLOW CALCULATED FROM EQ. 7.3, REF.1

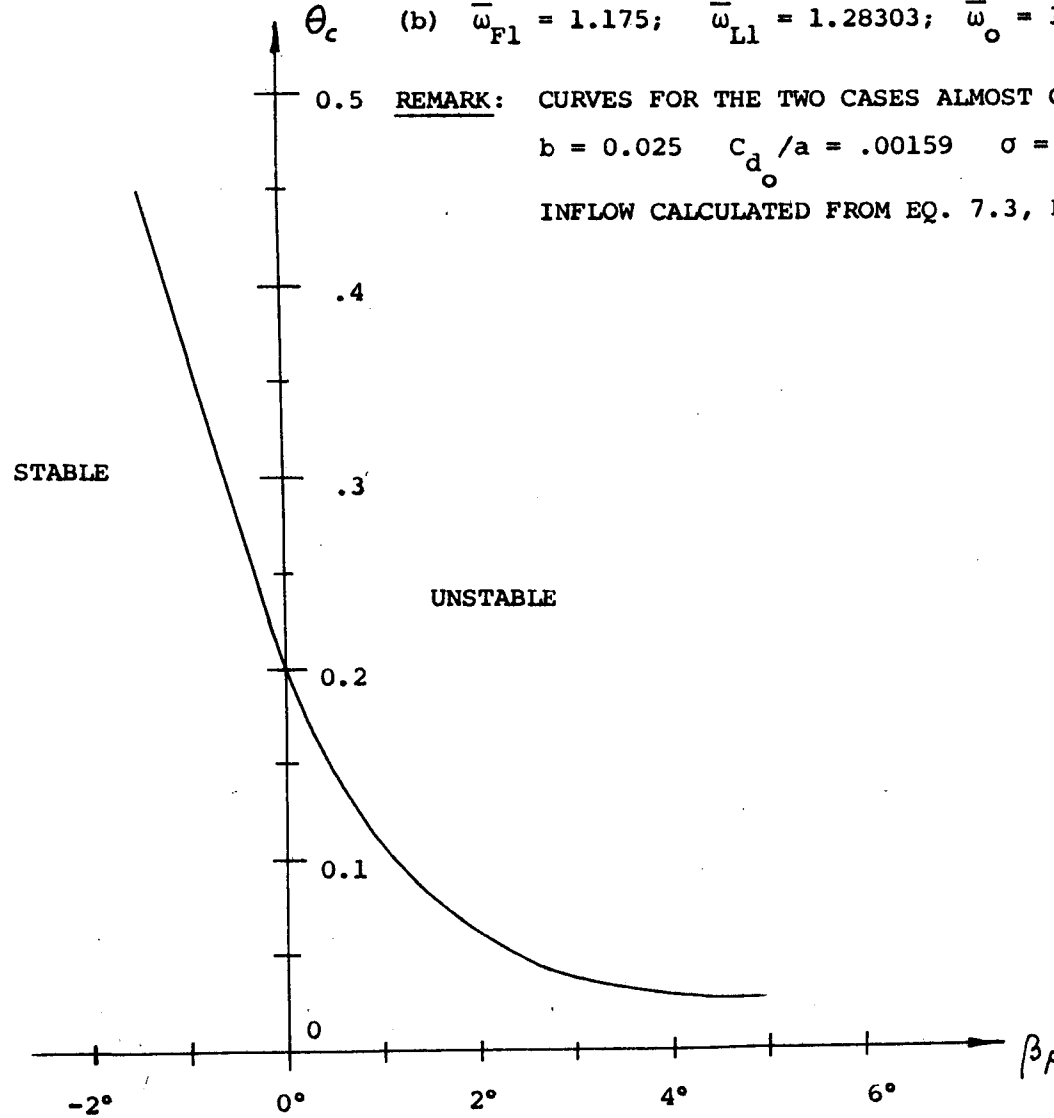


FIG. 4 EFFECT OF BUILT-IN CONING ON THE FLAP-LAG-TYPE OF STABILITY BOUNDARY